RESEARCH ARTICLE

Heterogeneity and Phenotypic Plasticity of Glial Cells in the Mammalian Enteric Nervous System

Werend Boesmans,[1] Reena Lasrado,[2] Pieter Vanden Berghe,[1] and Vassilis Pachnis[2]

Enteric glial cells are vital for the autonomic control of gastrointestinal homeostasis by the enteric nervous system. Several different functions have been assigned to enteric glial cells but whether these are performed by specialized subtypes with a distinctive phenotype and function remains elusive. We used Mosaic Analysis with Double Markers and inducible lineage tracing to characterize the morphology and dynamic molecular marker expression of enteric GLIA in the myenteric plexus. Functional analysis in individually identified enteric glia was performed by Ca^{2+} imaging. Our experiments have identified four morphologically distinct subpopulations of enteric glia in the gastrointestinal tract of adult mice. Marker expression analysis showed that the majority of glia in the myenteric plexus co-express glial fibrillary acidic protein (GFAP), S100β, and Sox10. However, a considerable fraction (up to 80%) of glia outside the myenteric ganglia, did not label for these markers. Lineage tracing experiments suggest that these alternative combinations of markers reflect dynamic gene regulation rather than lineage restrictions. At the functional level, the three myenteric glia subtypes can be distinguished by their differential response to adenosine triphosphate. Together, our studies reveal extensive heterogeneity and phenotypic plasticity of enteric glial cells and set a framework for further investigations aimed at deciphering their role in digestive function and disease.

GLIA 2014;00:000–000

Key words: enteric glia, enteric nervous system, neural crest, Ca^{2+} imaging

Introduction

Glial cells are essential for the organization and function of the nervous system (Jessen, 2004). In addition to their "traditional" roles in providing nourishment and support for neurons, glial cells regulate synaptic transmission, maintain the blood-brain barrier, mediate communication between the nervous and immune systems and monitor the nutritional state of organisms (Allaman et al., 2011; Giaume et al., 2010; Perea et al., 2009). Highlighting their critical role during embryogenesis and in postnatal life, several developmental, degenerative, and inflammatory disorders of the nervous system have been associated with deficits in glial cell function (Barres, 2008; Lee et al., 2000; Lemke, 2001). Enteric glial cells (EGCs) constitute a major population of peripheral glia that is located within the ganglia of the myenteric and submucosal plexus of the enteric nervous system (ENS) and in extraganglionic sites, such as the smooth muscle layers and the mucosa (Gershon and Rothman, 1991; Gulbransen and Sharkey, 2012; Ruhl et al., 2004). A series of studies has demonstrated that EGCs are critical for the regulation of gut motility, the secretory and absorptive functions of the intestinal epithelium and the host's defense against pathogens (De Giorgio et al., 2012; Gulbransen and Sharkey, 2012; Neunlist et al., 2013). Enteric neurons and EGCs are derived from neural crest cells which emerge during embryogenesis from the vagal and sacral level of the neural tube and colonize

View this article online at wileyonlinelibrary.com. DOI: 10.1002/glia.22746

Published online Month 00, 2014 in Wiley Online Library (wileyonlinelibrary.com). Received June 2, 2014, Accepted for publication Aug 5, 2014.

Address correspondence to P. Vanden Berghe, Laboratory for Enteric Neuroscience (LENS), TARGID, O&N1 #701, University of Leuven, Herestraat 49, 3000 Leuven, Belgium. Phone: +3216330153; Fax: +3216345939. E-mail: pieter.vandenberghe@med.kuleuven.be and to V. Pachnis, Division of Molecular Neurobiology, MRC National Institute for Medical Research, The Ridgeway, Mill Hill, London, NW7 1AA, UK. Phone: +442088162113; Fax: +442088162109. E-mail: vpachni@nimr.mrc.ac.uk

From the [1]Laboratory for Enteric NeuroScience (LENS), TARGID, Department of Clinical and Experimental Medicine, University of Leuven, Leuven, Belgium; [2]Division of Molecular Neurobiology, MRC National Institute for Medical Research (NIMR), London, United Kingdom.

Werend Boesmans and Reena Lasrado have contributed equally to this work.

Pieter Vanden Berghe and Vassilis Pachnis are co-corresponding senior authors.

Additional Supporting Information may be found in the online version of this article.

uniformly the entire length of the gastrointestinal tract (Heanue and Pachnis, 2007; Sasselli et al., 2012). Although diversity of enteric neuron subtypes has been studied intensively in mammals (Furness, 2000), our understanding of the extent, the origin and physiological significance of EGC diversification remains unclear. Pioneering work from Hanani and Reichenbach (1994) proposed a classification scheme for EGCs that was based on cell morphology and location within the plexus. However, the recognition that essential subsets of EGCs are located outside the ENS plexus, the advent of genetic tools that allow detailed characterization of EGCs and recent progress in understanding their physiological properties, warrant a reexamination of EGC subtype classification in a manner that takes into consideration morphological features, distribution within the gut wall as well as molecular and physiological attributes. Moreover, given that the gut constitutes one of the most dynamic organs of the body which adjusts constantly to the volatile microenvironment of the lumen (unpredictable availability of nutrients, changing populations of commensal bacteria, and exposure to pathogenic microorganisms), any classification scheme for EGCs must also consider the potential plasticity of subtypes identified at any given moment.

In the present study, we have carried out high resolution morphological characterization of EGC subtypes by combining Mosaic Analysis with Double Markers (MADM) with immunostainings for glial markers. In addition, we have examined the physiological properties of different subtypes of myenteric glia using Ca^{2+} imaging on live tissue. Furthermore, using Cre/LoxP technology we have carried out *in vivo* fate mapping and inducible lineage tracing of defined subsets of EGCs with the aim of exploring their plasticity in the myenteric ganglia. Our experiments extend previous studies on the morphological and physiological characterization of EGCs and highlight a novel subtype of extraganglionic glia which is located within the plexus. Moreover, our experiments have revealed previously unrecognized plasticity in the molecular phenotype of defined glial subpopulations of the mammalian ENS.

Materials and Methods

Animals

All experimental procedures were carried under a UK Home Office Project license and approved by the local Animal Ethics Committees of the National Institute of Medical Research and the University of Leuven. Animals were housed at an ambient temperature of 22°C–24°C on a 12:12 hr light/dark cycle. Drinking water and laboratory chow were provided *ad libitum*. The *Sox10::Cre* (Matsuoka et al., 2005), *MADM-6*^{GR} and *MADM-6*^{RG} (Zong et al., 2005), *hGFAP::-CreER*^{T2} (Ganat et al., 2006), and the *Rosa26R-YFP* (Srinivas et al., 2001) transgenic mice have been described previously. *In vivo* labeling of EGCs in *hGFAP::CreER*^{T2}; *Rosa26R-YFP* adult animals was achieved by intraperitoneal injections of 0.1–0.2 mg/g of 4-hydroxy tamoxifen (4-OHT; Sigma), which was dissolved in an ethanol/sunflower oil (1:9) mixture at 10 mg/mL (Laranjeira et al., 2011). Control mice were not injected or injected with an ethanol/sunflower oil (1:9) mixture.

Immunofluorescence of Adult Myenteric Plexus Preparations, Confocal Image Acquisition and Processing

Gut tissue was cut into 2 cm long pieces and mounted over a 1 mL pipette. An incision was made along the mesenteric border and a cotton swab soaked in PBS was used to roll out the longitudinal muscle with adherent myenteric plexus from the underlying tissue. Isolated adult myenteric plexus preparations were stretched and pinned onto Sylgard dishes (Sylgard 184 Elastomer, Dow Corning) using insect pins (0.2 mm, Agar Scientific) and fixed in ice-cold paraformaldehyde (4% in PBS) for 2 hr at 4°C. Fixed tissue samples were permeabilized in 0.3% TritonX-100 (Sigma) in PBS (PBT) and incubated in blocking solution (5% Normal Donkey Serum in PBT, Jacksons ImmunoResearch Laboratories). Primary antibodies (Table 1) were diluted in blocking solution and applied overnight at 4°C. Samples were washed in PBT and appropriate secondary antibodies were applied. The GFP antibodies were used to detect expression of the YFP reporter, and the two terms are used interchangeably. Secondary antibodies were goat or donkey hosted Alexa-Fluor 488, Alexa Fluor 568, Alexa Fluor 594, and Cy5 (all 1:500; Invitrogen and Jackson ImmunoResearch). Samples were mounted with Vectashield^{TM} mounting medium (Vector Labs).

Confocal and 3-D Images were acquired with Leica TCS SP5 (CIAL facility, NIMR, UK) and Zeiss LSM780 2-photon (Cell Imaging Core, KU Leuven) confocal microscopes using standard excitation and emission filters, assisted with Leica Application Suite Advanced Fluorescence (LAS AF) and Zeiss ZEN software, respectively. All images were processed with either Adobe Photoshop CS4 (Adobe Systems) or ImageJ (Wayne Rasband, NIH). 3-D reconstructions and morphological quantifications were obtained with Imaris 7.7 (Bitplane AG) after deconvolution using Huygens Professional (Scientific Volume Imaging).

Enteric Glial Cell Cultures

Primary cultures containing both enteric neurons and EGCs were prepared as described previously (Boesmans et al., 2013b). Briefly, tissue preparations of longitudinal muscle with adherent myenteric plexus were isolated from the ileum and collected in previously oxygenated Krebs solution (95% O_2 to 5% CO_2, 4°C). After washing, tissue preparations were digested in a collagenase (14.67 mg/mL)/protease (10 mg/mL)/albumin (5% in PBS) (Invitrogen) mixture for 8 min at 37°C. After stopping the enzymatic digestion by adding a Krebs solution with 10% foetal bovine serum (FBS) and washing by centrifugation the pellet was resuspended in medium (DMEM F-12) enriched with 10% FBS, 1% glutamine and 0.5% pen/strep (Lonza Group Ltd). The cells were plated on glass coverslips coated with poly-D-lysine hydro bromide (0.5 mg/ml in borate buffer) and laminin (20 μg/ml in PBS) (Sigma) and cultured at 37°C (95% O_2 to 5% $CO_{2)}$. After 24 hr, the medium was replaced by a serum-free medium supplemented with nerve growth factor (0.05%, Alomone Laboratories), N2 (0.2%), and G5 (0.2%) (Invitrogen).

TABLE 1: Primary Antibodies Used for Immunofluorescence Labeling

Antigen	Host	Dilution	Source
S100β	Rabbit	1:500	DAKO
GFAP	Rabbit	1:500	DAKO
GFAP	Chicken	1:300	Abcam
Sox10	Goat	1:200	Santa Cruz Biotechnologies
GFP	Rabbit	1:1000	Invitrogen
GFP	Rat	1:1000	Nacalai Tesque
TuJ1	Mouse	1:1000	Covance
peripherin	Goat	1:500	Santa Cruz Biotechnologies
nNOS	Rabbit	1:400	Santa Cruz Biotechnologies
neurofilament-200	Chicken	1:500	Abcam
CD31	Rabbit	1:500	Abcam
myc	Goat	1:500	Novus Biologicals

Live Calcium Imaging

Ca^{2+} imaging of EGCs and subsequent analysis was performed as previously described (Boesmans et al., 2013b; Vanden Berghe et al., 2008). The proximal colon of MADM-$6^{GR/RG}$; *Sox10*-Cre mice was pinned flat in a Sylgard-lined dish filled with Krebs solution (bubbled with 95% O_2 to 5% CO_2) and the mucosa and longitudinal muscle layer were carefully removed. Myenteric plexus preparations were loaded with 1 μM Rhodamine 2 (Rhod2, RT, 20 min, TEFLabs) in Krebs with cremophor EL (0.01%, Fluka). During recordings, a constant flow (1 mL/min) of Krebs (with or without 10 μM ATP, Sigma) solution was maintained via a gravity-fed electronic valve system. 1 μM nifedipine (Sigma) was added to the Krebs solution to inhibit smooth muscle contractions. Images were recorded on an upright Axiovert 200M microscope (Zeiss) with a Poly V xenon monochromator (TILL Photonics) and water dipping lens (20X, 1.0 NA, Zeiss). MADM-induced GFP and Rhod2 were excited at 475 nm and 580 nm and captured at 525/50 nm (still) and 645/75 (at 2 Hz), respectively, on a Sensicam-QE CCD camera (PCO) using TillVisION (TILL Photonics). Calcium imaging analyses were performed with custom-written routines in Igor Pro (Wavematrics). Regions of interest were drawn, after which average Ca^{2+} signal intensity was calculated, normalized to the initial Rhod2 values and reported as $\Delta F/F_0$. Cells were considered as responders when the Rhod2 signal rose above baseline plus 3 times the intrinsic noise (standard deviation) during the recording.

Statistical Analysis

Analysis was performed on a total sample of cells (as reported) that were obtained from at least three animals per genotype or experimental condition. Differences between data sets were determined by ANOVA followed by Bonferroni *post-hoc* test (for multiple comparison tests). Chi-square or Fisher's exact tests were performed to compare proportions. A P value <0.05 was considered to be significant. Significant differences with $P < 0.05$, 0.01, and 0.001 were indicated with *, **, and ***, respectively. Statistical analysis was performed with Microsoft Excel (Microsoft) and GraphPad Prism (GraphPad Softwares). Error bars represent the standard error of the mean (SEM).

Results

High Resolution Labeling of EGCs Using Mosaic Analysis With Double Markers (MADM)

Glia-specific molecular markers that are expressed widely in the central and peripheral nervous system have been used extensively for the identification and characterization of EGCs in mouse embryos and adult animals. Among such markers are the intermediate filament glial fibrillary acidic protein (GFAP) and the Ca^{2+}-binding protein S100β, which are expressed by committed EGC progenitors and differentiated EGCs (Ferri et al., 1982; Jessen and Mirsky, 1980; Young et al., 2003). In addition to these cytoplasmic proteins, the nuclear localized transcription factor Sox10 is expressed by multipotential ENS progenitors (Bondurand et al., 2003; Paratore et al., 2002) and is maintained in immature and mature EGCs (Hoff et al., 2008; Laranjeira et al., 2011; Young et al., 2003). These markers, which are usually identified by immunostaining on fixed gut preparations, are either unsuitable for morphological characterization of EGCs (Sox10) or are expressed by contiguous glial cells thus precluding studies that require single cell resolution. We reasoned therefore that sparse labeling of EGCs with genetically encoded fluorescent reporters would facilitate high resolution

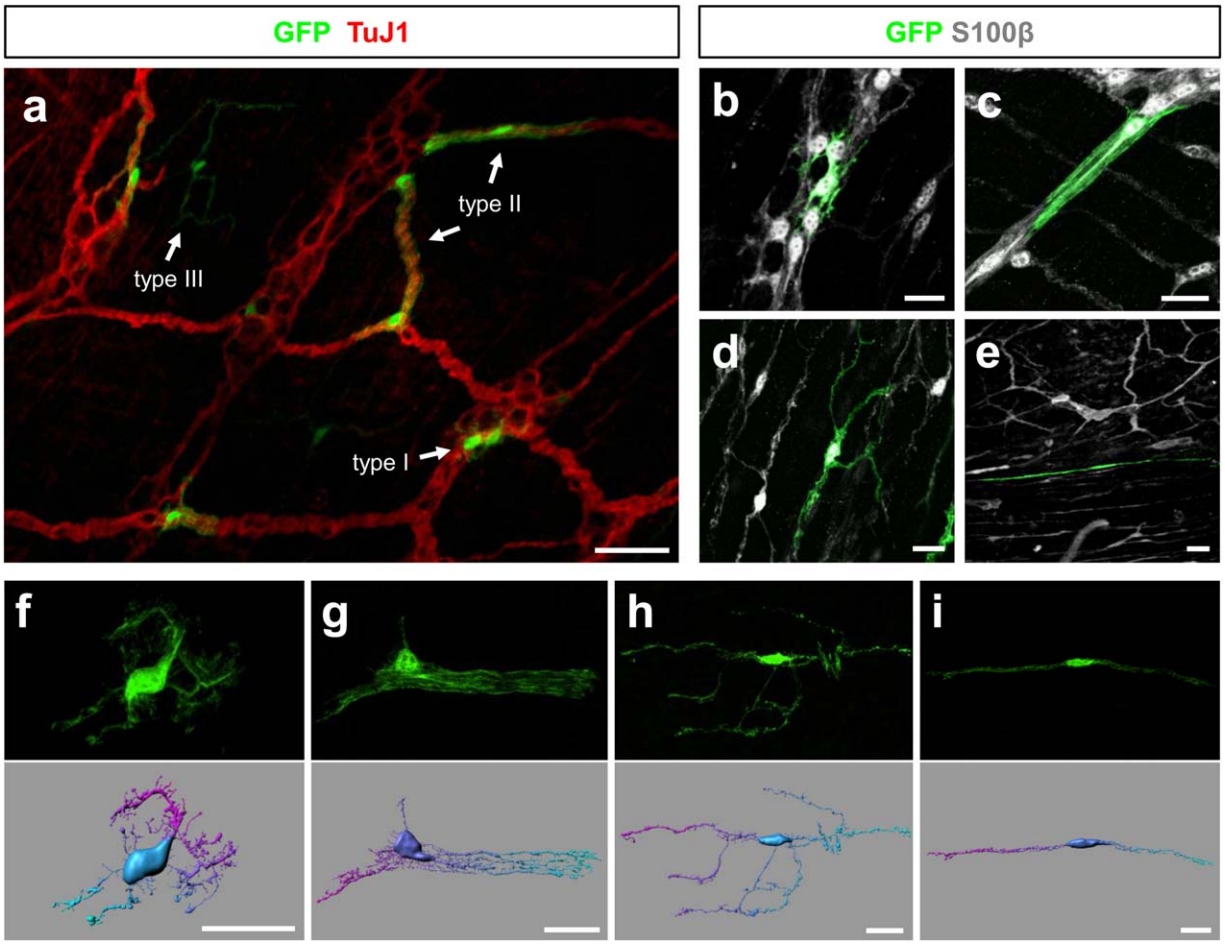

FIGURE 1: Single-cell labeling of enteric glia in Sox10Cre|MADM mice. (a) Individual EGCs expressing GFP (green) can be identified within and outside the ganglia and interconnectives of the myenteric plexus (Tuj1, red). (b–e) Double labeling of the different morphological subtypes of EGCs (type I–IV) expressing MADM-induced GFP (green) with the glial marker S100β (gray). (f–i) Deconvolved maximum projections (top) and 3-D reconstructions (bottom) of type I (f), II (g), III (h), and IV (i) EGCs identified in the ENS of Sox10Cre|MADM mice. See also Supp. Info. Movies 1–4. Scale bars: 50 μm (a), 20 μm (b–i). [Color figure can be viewed in the online issue, which is available at wileyonlinelibrary.com.]

morphological and physiological studies on both fixed and live tissue. To achieve this, we employed MADM, a sparsely labeling genetic system in which Cre-dependent interchromosomal recombination restores expression of fluorescent lineage tracers encoded by reciprocally chimaeric nonfunctional cassettes targeted to the same locus on homologous chromosomes (Zong et al., 2005). For our current studies we used the original MADM alleles (MADM-6^{GR} and MADM-6^{RG}) in which chimaeric GFP/RFP-Myc vectors have been inserted into the ubiquitously expressed *Rosa26* locus on mouse chromosome 6 (Zong et al., 2005). Introduction of the *Sox10::Cre* transgene, which drives expression of Cre recombinase in all neural crest cell lineages and peripheral glial cells (Laranjeira et al., 2011; Matsuoka et al., 2005), into MADM-6$^{GR/RG}$ compound heterozygous mice (designated hereafter Sox10-Cre|MADM), allowed us to mark with GFP or RFP-myc or both, isolated EGCs (Fig. 1a) and enteric neurons (which originate from marked Sox10$^+$ progenitors, Supp. Info. Fig. 1a). Since detection of RFP in Sox10Cre|MADM mice depends on immunostaining with anti-myc antibodies (Supp. Info. Fig. 1b), all studies reported here are based on the identification of GFP on fixed or live gut tissue preparations. The glial identity of all GFP$^+$ cells analyzed from Sox10Cre|MADM mice has been confirmed by double immunostaining with S100β-specific antibodies (Fig. 1b–e).

Characterization of GFP-expressing cells in whole-mount preparations of the different layers of the gut wall from Sox10Cre|MADM mice, allowed us to identify four EGC subtypes on the basis of morphology and location. Restricted within the ganglia of the myenteric and submucosal plexus were numerous GFP$^+$ cells bearing multiple irregular and highly branched processes which extended in all directions up to 42.5 ± 2.5 μm away from the cell body (Fig. 1b,f; Table 2; Supp. Info. Movie 1). The processes of

TABLE 2: Morphometric Analysis of Enteric Glia Subtypes[a]

	Type-I	Type-II	Type-III	Type-IV	One-way ANOVA
Cell body volume (μm^3)	335.4 ± 36.0	241.9 ± 15.4	275.7 ± 18.8	277.6 ± 44.5	$P = 0.0869$
Total cell volume (μm^3)	677.0 ± 97.2	699.5 ± 144.4	791.7 ± 60.4	490.0 ± 33.0	$P = 0.5547$
Average process length (μm)	30.9 ± 1.4	53.9 ± 6.1	87.6 ± 5.3	124.0 ± 11.4	$P < 0.0001$
Maximal process length (μm)	42.5 ± 2.5	77.6 ± 9.7	118.1 ± 8.2	138.1 ± 15.5	$P < 0.0001$
Largest cell axis (μm)	52.9 ± 4.2	88.0 ± 11.7	144.7 ± 10.8	229.0 ± 24.4	$P < 0.0001$

[a]Data are represented as average ± SEM.

these intraganglionic glial cells often terminate with "end-feet" like structures and were intermingled with processes from other neighboring EGCs and were contacting multiple neurons within the same ganglion (Fig. 2a; Supp. Info. Movie 2). These astrocyte-like glial cells correspond to the "protoplasmic" or type-I EGCs described previously by Hanani and Reichenbach (1994). These authors provided also the first description of the "fibrous" or type-II EGC found within or at the edges of the interganglionic connectives. Using GFP expression as marker, we have confirmed that this EGC subtype has lanky processes that emerge mostly from one side of the cell and run for 53.9 ± 6.1 μm in parallel to each other and to the neuronal fibers of the interganglionic strands (Fig. 1c,g; Table 2; Supp. Info. Movie 3). These glial cell processes contact most neural fibers but they do not wrap around them in a manner analogous to the ensheathing of peripheral nerve fibers by Schwann cells (Fig. 2b; Supp. Info. Movie 4). In addition to the type-I and type-II EGCs we have uncovered a morphologically distinct glial subtype which is at the level of the myenteric and submucosal plexus but lies outside the ganglia and the interganglionic connectives (Fig. 1a). This subtype, designated hereafter as type-III, exhibits mainly four major processes (87.6 ± 5.3 μm) with secondary branching (Fig. 1d,h; Table 2; Supp. Info. Movie 5). Type-III EGCs appear to form a matrix in the extraganglionic region, and remain in close association with neuronal fibers running along their processes (Fig. 2c). In addition, the processes of type-III EGCs are often seen wrapping around small blood vessels (Fig. 2d). EGCs with a similar morphology have been described previously as a distinct subtype within the lamina propria of the mucosa and have been termed "mucosal" or type-III EGCs (Gulbransen and Sharkey, 2012; Savidge et al., 2007). Given their morphological similarities but distinct location, we propose to discriminate between the mucosal and plexus positioned type-III EGCs by referring to them as type-III_{Mucosa} and type-$III_{MP/SMP}$ respectively. Finally, our MADM labeling system also revealed EGCs with a characteristic bipolar morphology which were located within the circular and longitudinal smooth muscle layers along nerve fibers (Fig. 1e,i; Table 2; Supp. Info. Movie 6). These cells correspond to the type-IV EGCs described previously (Gulbransen and Sharkey, 2012; Vanderwinden et al., 2003). Taken together, our experiments extend previous studies on the classification of EGCs and demonstrate that MADM-mediated fluorescent labeling can be used effectively for high resolution morphological analysis of individual glial cells throughout the mammalian ENS. All our subsequent studies were carried out on glial cells (types I–III) of the myenteric plexus.

Differential Expression of Glial Markers in Subtype Populations of Myenteric Glia

So far, the markers GFAP, S100β, and Sox10 have been used interchangeably for the identification of EGCs. To determine whether the EGC subtypes within the myenteric plexus can be distinguished by the differential expression of these commonly used glial markers, we performed double immunostaining of myenteric plexus preparations isolated from the intestine of P90 mice using combinations of marker-specific antibodies. First, we quantified the expression of GFAP and S100β. Whereas, the majority of type-I EGCs residing in the myenteric ganglia co-expressed GFAP and S100 ($GFAP^+/S100\beta^+$; 55.8 ± 5.2%), the remainder cells of this subtype population expressed either S100β ($GFAP^-/S100\beta^+$; 29.9 ± 4.4%) or GFAP ($GFAP^+/S100\beta^-$; 14.3 ± 3.9%) only (Fig. 3a,b). Interestingly, the percentage of $GFAP^-/S100\beta^+$ cells among the type-II and type-III_{MP} EGCs was significantly higher (59.6 ± 1.6% and 78.9 ± 0.7%, respectively) relative to that in type-I glia. Notably, a relatively high percentage of $GFAP^+/S100\beta^-$ cells (~50%) displayed remarkably high immunoreactivity for GFAP (Fig. 3a, arrow). Next, we compared the expression of GFAP and Sox10. Similar to our findings with the GFAP/S100β combination, in all three EGC subtypes we identified cells that expressed either one or both of these markers. Thus, 74.4 ± 2.4% of the type-I glia were $GFAP^+/Sox10^+$ but only 19.3 ± 1.5% were $GFAP^-/Sox10^+$ and 6.2 ± 0.9% expressed only GFAP (Fig. 3c,d). In type-II EGCs

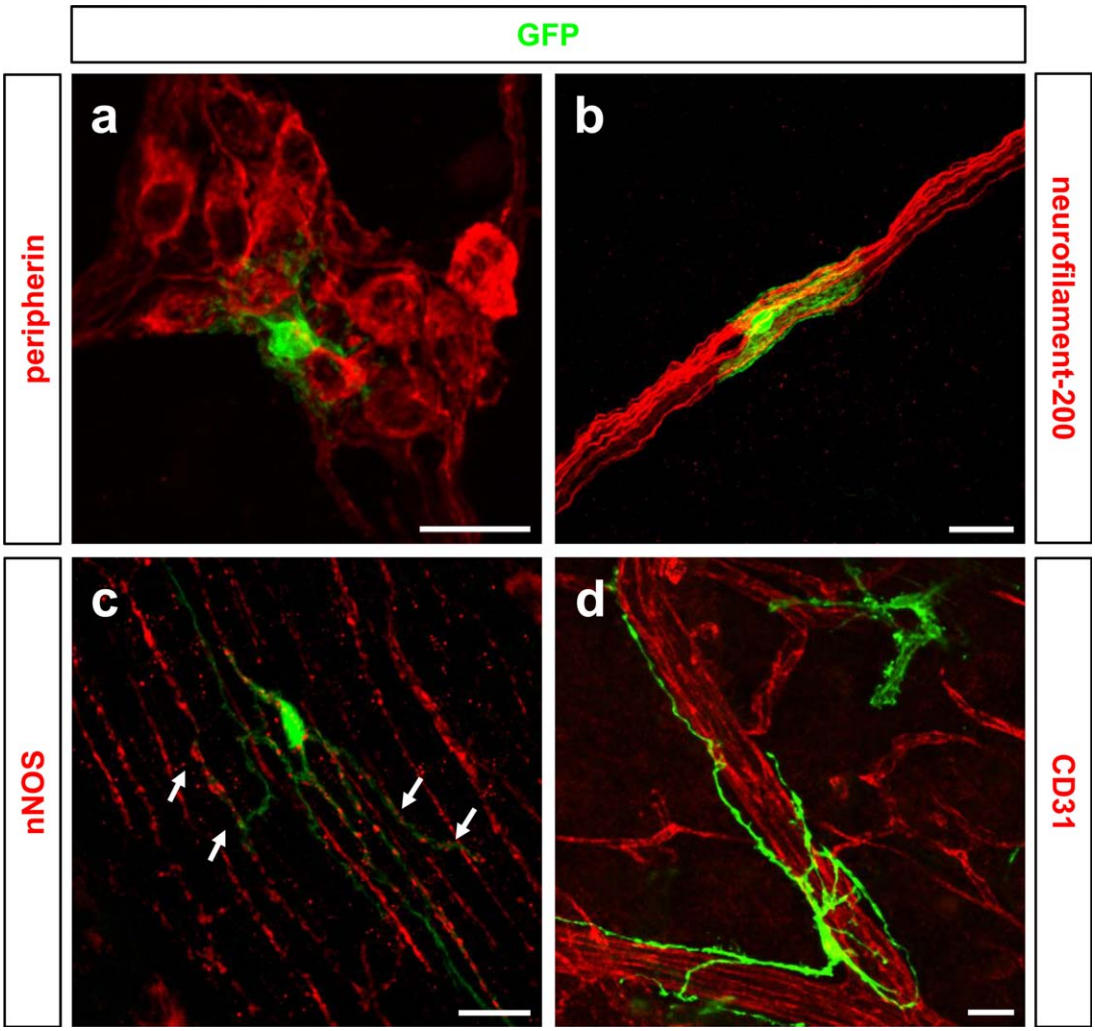

FIGURE 2: Interaction between enteric neurons and glia in the myenteric plexus of Sox10Cre|MADM mice. (a) Type-I EGC (green) in close apposition with enteric neurons labeled for the pan-neuronal marker peripherin (red) within a myenteric ganglion. (b) Type-II EGC (green) located in an interganglionic connective positive for neurofilament-200 (red). (c) Type-III EGC (green) positioned at the level of the myenteric plexus with several of its processes contacting nitrergic (nNOS, red) nerve fibers and varicosities (arrows). (d) Type-III EGC (green) wrapping around a blood vessel (CD31, red). See also Supp. Info. Movies 5 and 6. Scale bars: 20 μm. [Color figure can be viewed in the online issue, which is available at wileyonlinelibrary.com.]

the percentage of $GFAP^-/Sox10^+$ cells increased to 46.4 ± 3.7% at the expense mostly of the double positive population, whereas in type-III_{MP} glia it increased further to 67.6 ± 5.1% at the expense of both the double positive and the GFAP-only population (Fig. 3d). The relative percentage of $GFAP^-/Sox10^+$ cells observed in the three types of glial cells mirrors the relative percentage of $GFAP^-/S100\beta^+$ glia (Fig. 3b) suggesting that the majority of $S100\beta^+$ glial cells co-express Sox10. This was confirmed by double immunostaining with a combination of S100β and Sox10 antibodies which demonstrated that virtually all $S100\beta^+$ cells co-expressed Sox10 (Fig. 3e,f). Nevertheless, a small population of type-I (5.5 ± 1.5%) and type-II (7.4 ± 1.4%) glia expressed only Sox10 ($S100\beta^-/Sox10^+$) and this fraction increased slightly in type-III_{MP} EGCs (10.7 ± 1.9%, Fig. 3f). Taken together, these data indicate that none of the markers examined here (and commonly used for the identification of EGCs) can uniquely identify any of the morphologically distinct glial subtypes within the myenteric plexus. Nevertheless, the differential abundance of cells expressing combinations of GFAP, S100β, and Sox10 within the glial subtypes I–III of the myenteric plexus suggests that glia-specific gene expression in the mammalian gut is highly dynamic and is influenced *at the population level* by spatially and temporally controlled factors.

Differential Response of EGC Subtypes to Purinergic Activation

To investigate whether, in addition to the differential marker expression, EGC subtypes are also characterized by distinct physiological properties, we performed Ca^{2+} imaging

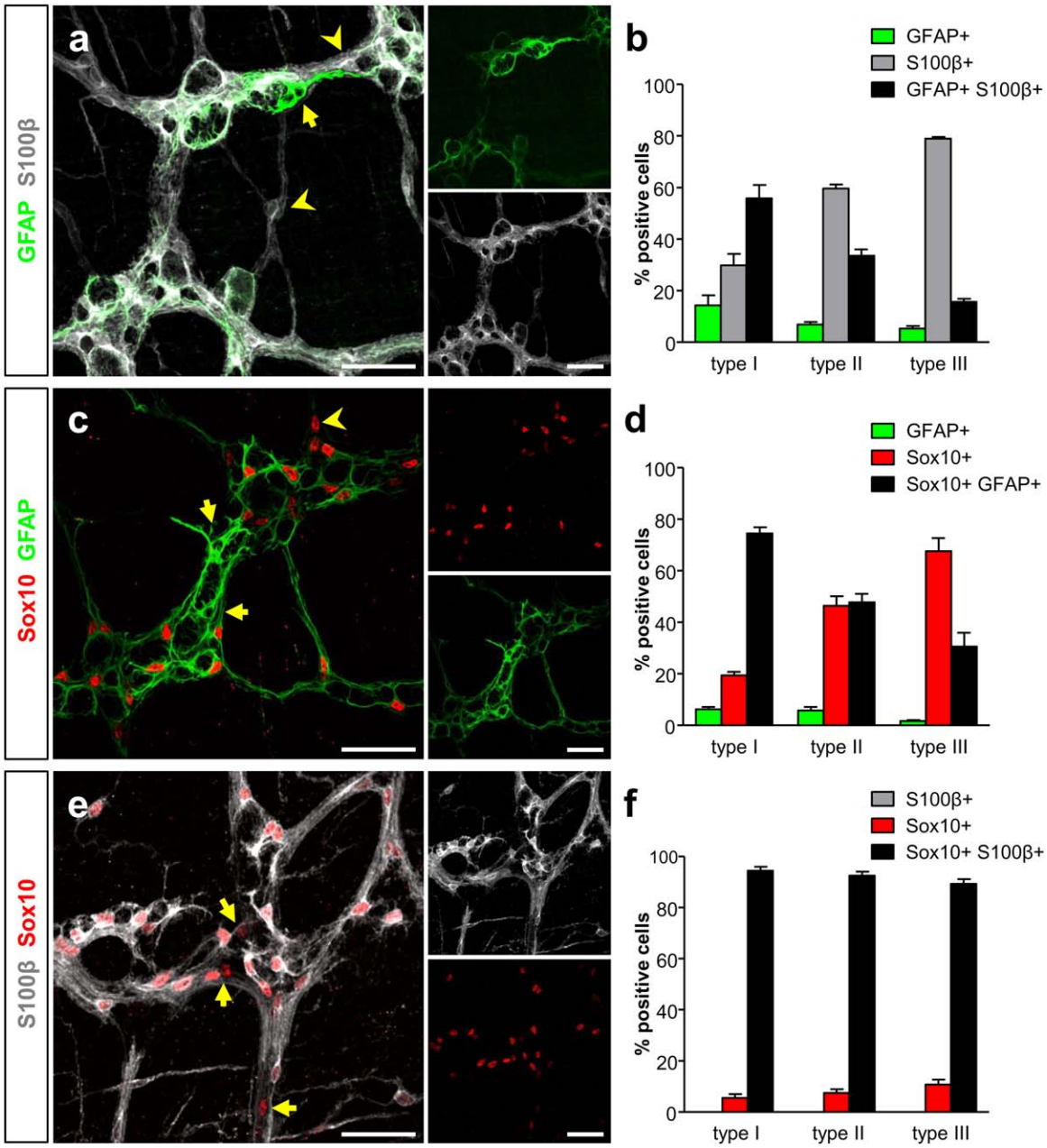

FIGURE 3: Differential expression of GFAP, S100β, and Sox10 in enteric glia of the myenteric plexus of the ileum. (a) Double immunostaining for GFAP (green) and S100β (gray). Although most EGCs express both markers, EGCs only positive for GFAP (arrow) or S100β (arrowheads) can be observed. (c) Double immunostaining for GFAP (green) and Sox10 (red). Note the presence of EGCs expressing only GFAP (arrows) or Sox10 (arrowhead). (e) Double immunostaining for S100β (gray) and Sox10 (red). The majority of cells were found positive for both S100β and Sox10. A small proportion of cells positive for Sox10 did not express S100β (arrows). EGCs positive for S100β but not for Sox10 were not observed. (b, d, f) Quantification of single and double positive cells in the different subtype populations of EGCs in the myenteric plexus (Chi-square: b: $P < 0.0001$, d: $P < 0.0001$, f: $P = 0.0388$). A total of 1,851 (b), 2,420 (d), and 1,792 (f) cells were counted per co-staining. Scale bars: 50 μm. [Color figure can be viewed in the online issue, which is available at wileyonlinelibrary.com.]

experiments on fresh preparations of myenteric plexus. Given the established paradigm of purinergic neuron-to-glia communication in the ENS (Boesmans et al., 2013b; Gomes et al., 2009; Gulbransen and Sharkey, 2009), we decided to test whether the three myenteric glia subtypes respond differently to purinergic receptor stimulation. For this, we loaded myenteric plexus preparations dissected from Sox10Cre|MADM mouse colon with the red Ca^{2+} indicator Rhodamine-2. This enabled us to unambiguously measure the changes in intracellular Ca^{2+} concentration upon ATP (10 μM, 20 s) stimulation in individual cells that belong to the three EGC subtypes of the myenteric plexus (Fig. 4). We found that the majority (86.8%) of intraganglionic type-I EGCs respond with a Ca^{2+} transient ($\Delta F/F_0$: 7.0 ± 0.9%) when challenged with

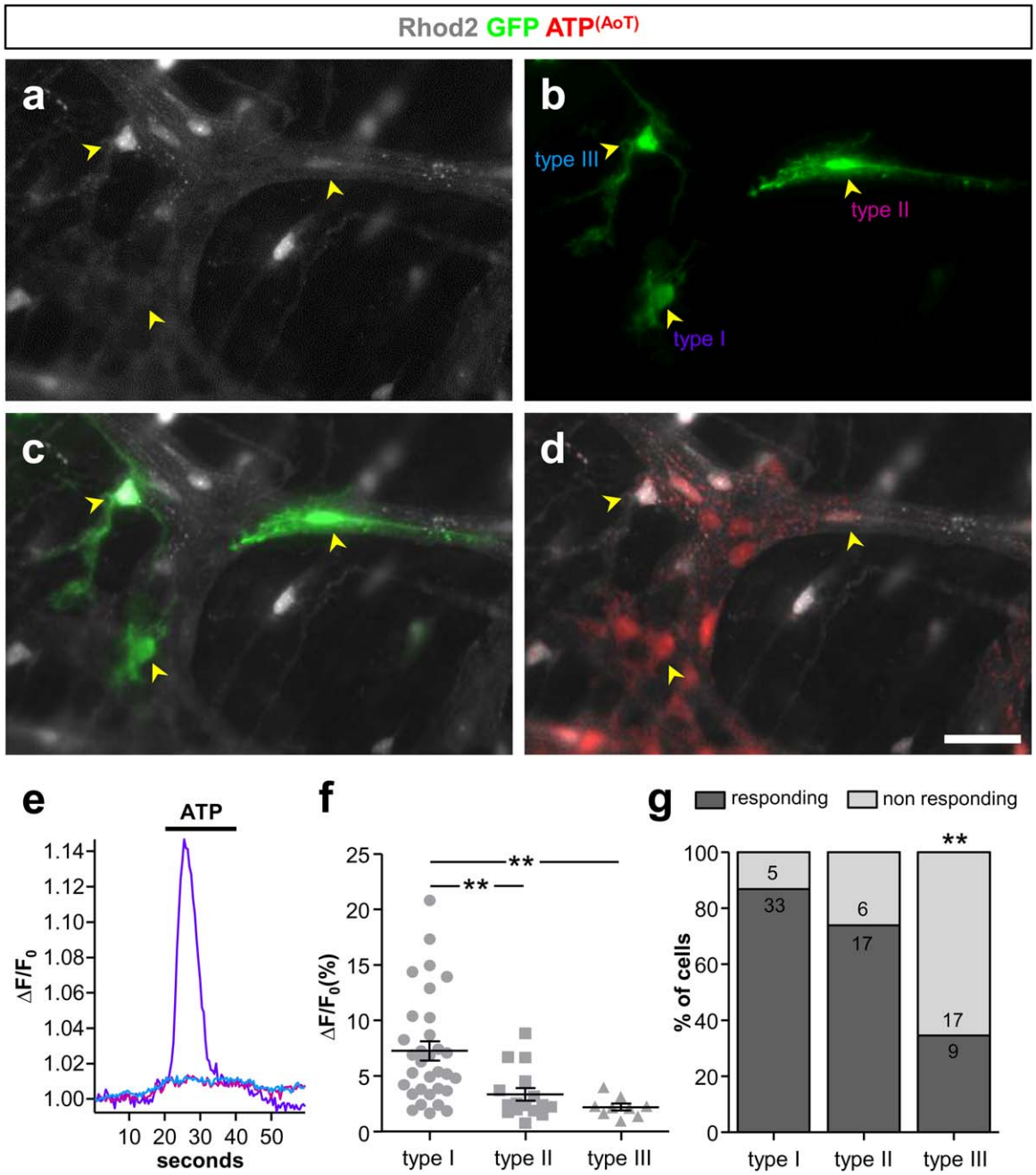

FIGURE 4: Intracellular Ca^{2+} imaging in individually identified enteric glia. (a–d) Representative images of a myenteric plexus preparation isolated from a Sox10Cre|MADM mouse and loaded with the fluorescent Ca^{2+} indicator Rhodamine-2 (Rhod2, a) that illustrate the three subtypes of EGCs in the myenteric plexus (arrowheads) expressing GFP (b, c). Cells responding to ATP stimulation (10 μM, 20 s, d) were falsely colored in red by an activity-over-time operation. (e) ATP-evoked $[Ca^{2+}]_i$ response of GFP-expressing cells depicted in (a–d, arrowheads, color-coded Rhod2 traces match the three subtypes depicted in (b). (f) Maximal amplitude of the ATP-induced Ca^{2+} transient in the three morphologically different subtypes (ANOVA: $P = 0.0004$, **Bonferonni *post-hoc*). (g) Proportion of cells that displayed (or not) a Ca^{2+} transient upon ATP stimulation (Fisher's exact). The total number of cells responding and nonresponding to ATP is shown. Scale bar: 20 μm. [Color figure can be viewed in the online issue, which is available at wileyonlinelibrary.com.]**

ATP (Fig. 4d–g). Although purinergic receptor stimulation induced Ca^{2+} rises in a similar proportion (73.9%) of type-II EGCs in the interconnectives fiber tracts, Ca^{2+} transient amplitudes were significantly lower ($\Delta F/F_0$: 3.1 ± 0.6%) (Fig. 4f,g). Among type-III_{MP} EGCs located in the interganglionic space, only 34.6% displayed Ca^{2+} rises ($\Delta F/F_0$: 1.9 ± 0.3%) upon ATP stimulation (Fig. 4f,g). Thus, compared to type-I and type-II EGCs, extraganglionic type-III_{MP} cells display a decreased responsiveness to purinergic receptor stimulation. These data are consistent with our

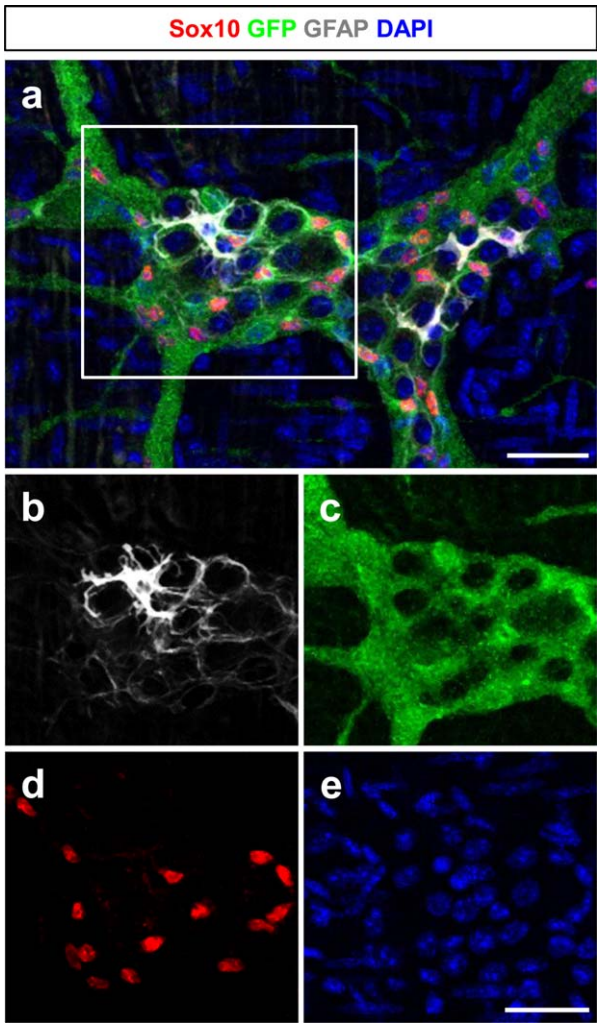

FIGURE 5: Sox10$^-$ and Sox10$^+$ enteric glia are derived from a common pool of Sox10 expressing progenitors. (a) Maximum projection of a myenteric plexus preparation derived from a Sox10Cre|YFP mouse immunostained for YFP (green), Sox10 (red), and GFAP (gray), and counterstained with DAPI (blue). Inset shows a Sox10$^-$/GFAP$^+$ cell. (b–e) Break up of panels showing the cell depicted in the inset in (a). Scale bars: 50 μm (a), 20 μm (b–e). [Color figure can be viewed in the online issue, which is available at wileyonlinelibrary.com.]

morphological analysis and argue that the constituent populations of EGCs in the myenteric plexus can be distinguished on the basis of neurotransmitter responses.

Sox10 Negative EGCs are Derived From Sox10-Expressing Progenitors

Since Sox10 is known to mark all glia of the peripheral nervous system (Herbarth et al., 1998; Pusch et al., 1998), we were surprised to identify a small but readily detectable population of GFAP-expressing EGCs that were negative for this transcription factor (Fig. 3c,d). This subset of EGCs could be derived either from a previously uncharacterized Sox10$^-$ cell lineage or from Sox10$^+$ precursors that down-regulate expression of *Sox10* upon terminal differentiation. To distinguish between these possibilities, we used Cre/LoxP technology to fate map Sox10-expressing ENS progenitors *in vivo*. More specifically, we combined the *Sox10::Cre* transgene, which drives expression of Cre recombinase in all neural crest cell lineages, with the Cre-dependent reporter *Rosa26-ReYFP* (Laranjeira et al., 2011; Matsuoka et al., 2005). Expression of *Sox10* in these mice (called hereafter Sox10Cre|YFP) would be accompanied by induction of Cre and permanent activation of the *Rosa26-ReYFP* reporter irrespective of the continued activity of the *Sox10* locus. By analyzing preparations of the myenteric plexus from P90 Sox10Cre|YFP mice, we found that the majority (95.7%, 47 cells) of Sox10$^-$/GFAP$^+$ cells expressed YFP, indicating that they are derived from Sox10$^+$ progenitors (Fig. 5). These data confirm that all populations of EGCs in the myenteric plexus are derived from Sox10-expressing progenitors and suggest that the expression of characteristic marker genes in EGC lineages can be highly dynamic. The latter was confirmed when double immunostaining for GFAP, S100β, and Sox10 was performed on primary cultured EGCs derived from the myenteric plexus (Supp. Info. Fig. 2). Although we found that the levels of GFAP immunoreactivity did vary between individual cells in culture, EGCs expressing only one of the markers were not observed after 4 days *in vitro*. Thus, when EGCs are isolated from their natural environment, and their spatial interactions with other cell types in the gut wall are lost, they can no longer be distinguished based on their expression of GFAP, S100β, or Sox10. Taken together, our experiments support the phenotypic plasticity of EGC subtypes.

Dynamic Expression of GFAP in EGCs

Up-regulation of GFAP is one of the main features of reactive astrogliosis, a hallmark of several central nervous system pathologies (Sofroniew, 2009). In the ENS, increased GFAP expression has been demonstrated in inflammatory bowel disease patients, in mouse EGCs following ischemia and in cytokine-treated cultures of rat EGCs (Cornet et al., 2001; Thacker et al., 2011; von Boyen et al., 2004). Variation in the levels of GFAP expression is also illustrated by the different grades of GFAP immunoreactivity that we have observed mostly in type-I EGCs (Fig. 3a,b). Although these studies suggest a certain degree of plasticity in the molecular phenotype of EGCs, direct evidence for a temporal regulation of glial-specific cell markers at the single-cell level in the ENS of adult animals is currently not available. In addition, it remains unclear whether the differential expression of GFAP marks distinct sublineages of EGCs or represent mere fluctuations in the levels of this protein in response to cell intrinsic or environmental changes. To address these issues, we used Cre/LoxP technology to follow over a period of several

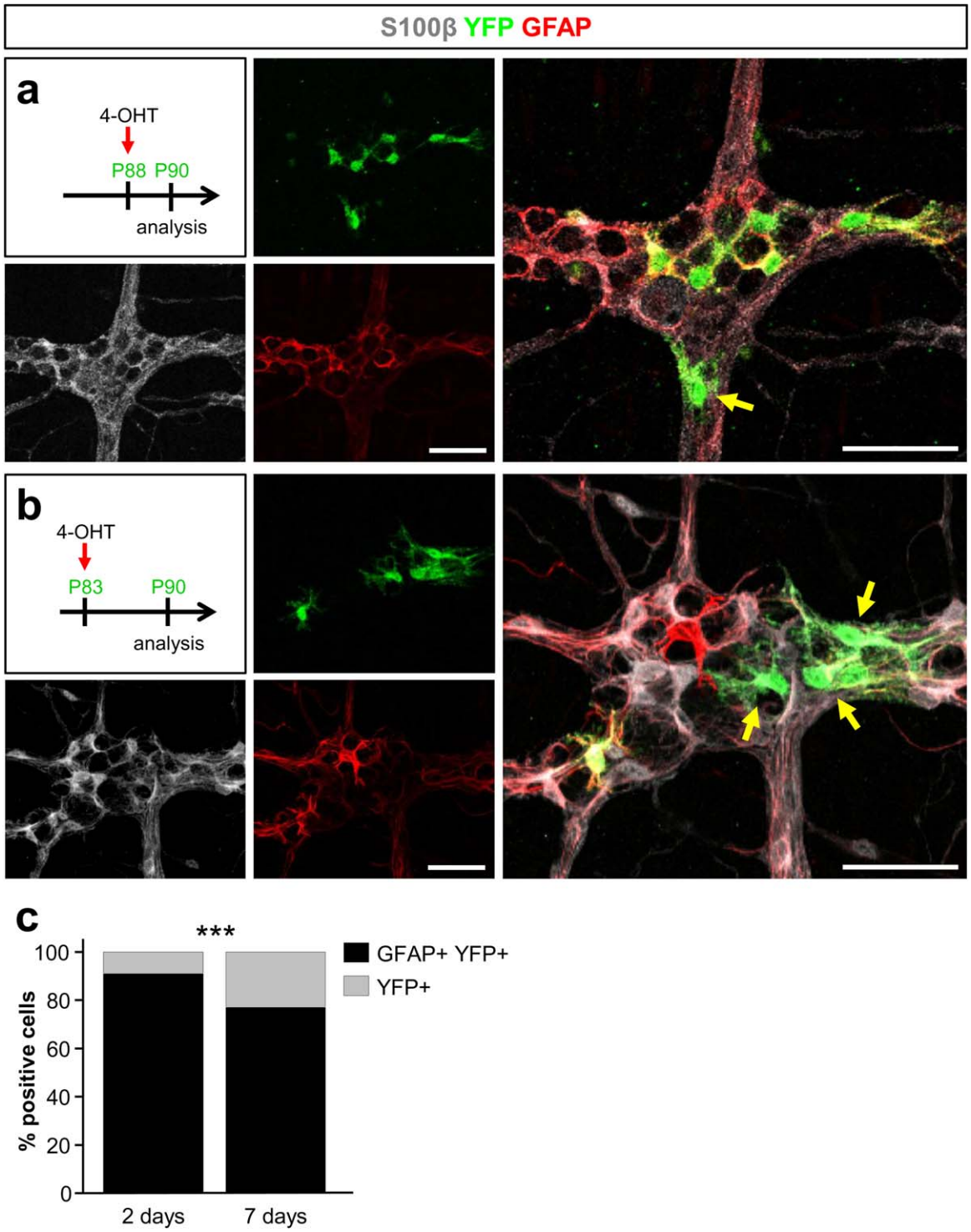

FIGURE 6: GFAP expression is highly dynamic in individual enteric glia. (**a, b**) Representative maximum projection of a myenteric plexus preparation isolated from a GFAPCreER|YFP mouse in which 4-OHT was administered 2 (a) or 7 (b) days prior to tissue collection and immunostaining for S100β (gray), YFP (green), and GFAP (red). Arrows points to YFP expressing cells that were not labeled by immunostaining for GFAP. (**c**) Quantification of single (YFP^+) and double ($GFAP^+/YFP^+$) positive cells 2 or 7 days after 4-OHT administration (***Fisher's exact). A total of 164 (a) and 316 (b) cells were counted per experiment. Scale bars: 50 μm. [Color figure can be viewed in the online issue, which is available at wileyonlinelibrary.com.]

days the potential change in GFAP expression in a defined population of $GFAP^+$ EGCs. More specifically, mice heterozygous for the *hGFAP::CreER^{T2}* transgene, which drives expression of tamoxifen-inducible Cre recombinase under the control of the human GFAP promoter (Ganat et al., 2006), and the Cre-dependent *Rosa26-ReYFP* reporter (mice called GFAPCreER|YFP), were administered 4-OHT and expression of GFAP in YFP^+ cells was analyzed in myenteric plexus preparations 2 and 7 days later. As expected, 2 days after 4-OHT administration, the vast majority of YFP^+ EGCs (91%) was also positive for GFAP (Fig. 6a). Interestingly, similar analysis 7 days following 4-OHT injection showed that only 77% of YFP^+ cells co-expressed GFAP (Fig. 6b). Since the percentage of $GFAP^+$ cells in the myenteric ganglia of adult animals remains constant (Joseph et al., 2011; Stenkamp-Strahm et al., 2013), these experiments suggest that under physiological conditions expression of GFAP in *individual* EGCs varies considerably over time.

Discussion

Traditionally, EGCs were thought to contribute primarily to the structural integrity and nourishment of the ENS. However, during the last decades several studies have confuted the concept of a merely supportive function of EGCs and ascribed to them a wide variety of roles that are essential for proper gastrointestinal function. Thus, in addition to being a scaffold for neurons, EGCs function in mucosal integrity, neuroprotection, adult neurogenesis, neuro-immune interactions, and synaptic transmission (De Giorgio et al., 2012; Gulbransen and Sharkey, 2012; Neunlist et al., 2013; Ruhl et al., 2004). Although different morphological subtypes of EGCs have been described previously (Hanani and Reichenbach, 1994), they are generally thought to represent manifestations of a molecularly and physiologically homogeneous multitasking cell population. Some differences in the expression of receptors, channels, and enzymes have been reported (Boesmans et al., 2013b, 2014; Costagliola et al., 2009; Nasser et al., 2007, 2006b; Tjwa et al., 2003), but so far no studies have addressed the intrinsic heterogeneity of the recognized subtypes of EGCs. Recent *in vivo* ablation models have advanced considerably our understanding of EGC function (Aube et al., 2006; Bush et al., 1998; Cornet et al., 2001; Nasser et al., 2006a), but tissue disruption that encompasses relatively large cell populations is likely to lead to general effects on gastrointestinal homeostasis thus making it very difficult to pinpoint the relative contribution of EGC subtypes to the impaired epithelial barrier, inflammation, and nerve defects that have been observed.

Here, we have employed a high resolution genetic marking technique which allowed us to label individual glial cells of the gastrointestinal tract *in situ* and characterize their morphological and physiological properties. Using this approach, we have extended previous morphological studies and propose that the complement of EGCs is subdivided into four subtypes which correspond to unique locations within the plexus and extraganglionic spaces. Although these subtypes share many of the molecular markers that have been used to identify glial cells throughout the nervous system, they can be distinguished by the prevalence of marker expression across different populations. In particular, GFAP, a marker used widely for the identification of peripheral glial cells including EGCs, is expressed primarily by type-I intraganglionic glial cells but the majority of type-II and type-III EGCs are negative for this marker. Although GFAP has been implicated in the morphological characteristics and adhesive properties of astrocytoma cells (Sofroniew and Vinters, 2010), it is currently unclear whether the differential distribution of this intermediate filament has a functional relevance or simply reflects the sensitivity of type-I EGCs to GFAP-inducing signals. Irrespective of the physiological relevance of GFAP expression, our data suggest that the morphologically distinct subsets of EGCs express unique combinations of glial cell markers in response to signals from their immediate microenvironment and/or as a result of functional specialization. Our molecular studies so far have employed standard glial cell markers that are widely expressed in other parts of the peripheral and central nervous system and which have been used extensively in the ENS field. Systematic characterization of the molecular profile of EGC subtypes is likely to uncover unique combinations of additional molecules that can be used for the further classification and study of EGCs. Combinatorial codes of marker molecules emerging from such studies will assist considerably further investigations on the roles of EGCs in normal gut physiology and pathophysiology.

Heterogeneity among EGC subtypes could be developmentally hard-wired by the differentiation of distinct glial cell lineages emerging during embryogenesis. Alternatively, the different subtypes of EGCs could originate from the same glial cell precursors which, depending on their final destination, could give rise to morphologically and functionally distinct cell progeny. Developmental studies so far have failed to identify distinct progenitors of EGCs and the markers used so far are thought to label interchangeably a common progenitor (Heanue and Pachnis, 2007; Sasselli et al., 2012). Moreover, our lineage studies here argue for a considerable degree of phenotypic plasticity among EGC subtypes in adult animals. Taken together, these findings support a model according to which all subtypes of EGCs originate from a common progenitor which, depending on its final location and physiological context is capable of generating different glial subtypes. Probably, the ability of glial cells to acquire different properties is not restricted to embryonic or early postnatal stages but is maintained throughout adult life pointing to a

previously unrecognized degree of phenotypic plasticity of the ENS. Given the high correlation between location of EGCs within the plexus and phenotypic properties, it is currently unclear whether the acquisition of new properties by glial cells in adult animals is associated with cell translocation between the different subdomains of the neuroglial networks of the gut. Irrespective of the underlying cellular mechanisms, our data indicate that EGCs are capable of adjusting their phenotypic and molecular characteristics in response to continuous challenges associated with nutrition, microbiota, mechanical factors, or disease.

Although the exact role of EGCs in the mechanisms controlling the physiological output of the gut wall such as peristalsis or secretion remains elusive (Broadhead et al., 2012; MacEachern et al., 2011), previous studies have shown that purines arising from both intrinsic enteric and sympathetic neurons are the principal mediators of neuron-to-glia communication in the ENS (Gomes et al., 2009; Gulbransen and Sharkey, 2009; Gulbransen et al., 2010). Our experiments provide further support to this model and highlight the plausible role of type-I EGCs in integrating paracrine neurogenic information and modulating neuronal activity within the myenteric plexus (Boesmans et al., 2013b; Gulbransen and Sharkey, 2009). Although Ca^{2+} imaging techniques convincingly prove the activation of glial cells, the functional consequences of intracellular Ca^{2+} rises in EGCs have yet to be established. Purinergic enteric neuron-to-glia signaling is believed to be mediated via the purinergic receptor subtype P_2Y_1 (Boesmans et al., 2013a; Gomes et al., 2009; Gulbransen et al., 2012) but it is currently unclear whether this receptor is not expressed by type-II and type-III EGCs. Irrespective of the molecular mechanisms, the lack of response to ATP by EGC subtypes II and III may reflect developmental immaturity of the latter cell populations. This idea is consistent with the reduced expression of GFAP in these subpopulations, a marker thought to be expressed generally by mature EGCs (Jessen and Mirsky, 1980). Further lineage tracing studies will be necessary to resolve these issues.

In conclusion, by combining genetic single-cell labeling, *in vivo* fate mapping and live Ca^{2+} imaging we provide evidence that EGCs can not only be discriminated on the basis of morphology and location but also display distinct molecular signatures and functional characteristics. Our studies set the basis for further exploring the heterogeneity among EGCs, which is a prerequisite to fully understand their role in gastrointestinal function and disease.

Author Contributions

Experiments, interpretation of data, drafting and editing of the manuscript were done by WB and RL. Study design, supervision, interpretation of data, editing of manuscript and acquisition of funding was performed by PVB and VP.

Acknowledgment

Grant sponsor: Medical Research Council (MRC, UK); Grant number: U117537087 (VP); Grant sponsor: Research Foundation Flanders (Fonds Wetenschappelijk Onderzoek; FWO); Grant number: G.0501.10 (PVB).

WB was supported by a postdoctoral fellowship from the FWO. We thank N. Kessaris and W. Richardson (*Sox10::Cre*), L. Luo (*MADM*) and M. Götz (*hGFAP::CreER^{T2}*) for providing valuable mouse strains. We also thank the members of the Pachnis lab and LENS for critical comments on the manuscript and useful discussions.

Conflict of Interest: The authors declare no conflict of interest.

References

Allaman I, Belanger M, Magistretti PJ. 2011. Astrocyte-neuron metabolic relationships: for better and for worse. Trends Neurosci 34(2):76–87.

Aube AC, Cabarrocas J, Bauer J, Philippe D, Aubert P, Doulay F, Liblau R, Galmiche JP, Neunlist M. 2006. Changes in enteric neurone phenotype and intestinal functions in a transgenic mouse model of enteric glia disruption. Gut 55(5):630–637.

Barres BA. 2008. The mystery and magic of glia: a perspective on their roles in health and disease. Neuron 60(3):430–440.

Boesmans W, Cirillo C, Van den Abbeel V, Van den Haute C, Depoortere I, Tack J, Vanden Berghe P. 2013a. Neurotransmitters involved in fast excitatory neurotransmission directly activate enteric glial cells. Neurogastroenterol Motil 25(2):e151–-160.

Boesmans W, Martens MA, Weltens N, Hao MM, Tack J, Cirillo C, Vanden Berghe P. 2013b. Imaging neuron-glia interactions in the enteric nervous system. Front Cell Neurosci 7:183.

Boesmans W, Rocha NP, Reis HJ, Holt M, Vanden Berghe P. 2014. The astrocyte marker Aldh1L1 does not reliably label enteric glial cells. Neurosci Lett 566:102–105.

Bondurand N, Natarajan D, Thapar N, Atkins C, Pachnis V. 2003. Neuron and glia generating progenitors of the mammalian enteric nervous system isolated from foetal and postnatal gut cultures. Development 130(25):6387–6400.

Broadhead MJ, Bayguinov PO, Okamoto T, Heredia DJ, Smith TK. 2012. Ca2+ transients in myenteric glial cells during the colonic migrating motor complex in the isolated murine large intestine. J Physiol 590(Pt 2): 335–350.

Bush TG, Savidge TC, Freeman TC, Cox HJ, Campbell EA, Mucke L, Johnson MH, Sofroniew MV. 1998. Fulminant jejuno-ileitis following ablation of enteric glia in adult transgenic mice. Cell 93(2):189–201.

Cornet A, Savidge TC, Cabarrocas J, Deng WL, Colombel JF, Lassmann H, Desreumaux P, Liblau RS. 2001. Enterocolitis induced by autoimmune targeting of enteric glial cells: a possible mechanism in Crohn's disease? Proc Natl Acad Sci USA 98(23):13306–13311.

Costagliola A, Van Nassauw L, Snyders D, Adriaensen D, Timmermans JP. 2009. Voltage-gated delayed rectifier K(v)1-subunits may serve as distinctive markers for enteroglial cells with different phenotypes in the murine ileum. Neurosci Lett 461(2):80–84.

De Giorgio R, Giancola F, Boschetti E, Abdo H, Lardeux B, Neunlist M. 2012. Enteric glia and neuroprotection: basic and clinical aspects. Am J Physiol Gastrointest Liver Physiol 303(8):G887–G893.

Ferri GL, Probert L, Cocchia D, Michetti F, Marangos PJ, Polak JM. 1982. Evidence for the presence of S-100 protein in the glial component of the human enteric nervous system. Nature 297(5865):409–410.

Furness JB. 2000. Types of neurons in the enteric nervous system. J Auton Nerv Syst 81(1–3):87–96.

Ganat YM, Silbereis J, Cave C, Ngu H, Anderson GM, Ohkubo Y, Ment LR, Vaccarino FM. 2006. Early postnatal astroglial cells produce multilineage precursors and neural stem cells in vivo. J Neurosci 26(33):8609–8621.

Gershon MD, Rothman TP. 1991. Enteric glia. Glia 4(2):195–204.

Giaume C, Koulakoff A, Roux L, Holcman D, Rouach N. 2010. Astroglial networks: a step further in neuroglial and gliovascular interactions. Nat Rev Neurosci 11(2):87–99.

Gomes P, Chevalier J, Boesmans W, Roosen L, van den Abbeel V, Neunlist M, Tack J, Vanden Berghe P. 2009. ATP-dependent paracrine communication between enteric neurons and glia in a primary cell culture derived from embryonic mice. Neurogastroenterol Motil 21(8):870-e62.

Gulbransen BD, Sharkey KA. 2009. Purinergic neuron-to-glia signaling in the enteric nervous system. Gastroenterology 136(4):1349–1358.

Gulbransen BD, Sharkey KA. 2012. Novel functional roles for enteric glia in the gastrointestinal tract. Nat Rev Gastroenterol Hepatol 9(11):625–632.

Gulbransen BD, Bains JS, Sharkey KA. 2010. Enteric glia are targets of the sympathetic innervation of the myenteric plexus in the guinea pig distal colon. J Neurosci 30(19):6801–6809.

Gulbransen BD, Bashashati M, Hirota SA, Gui X, Roberts JA, MacDonald JA, Muruve DA, McKay DM, Beck PL, Mawe GM, Thompson RJ, Sharkey KA. 2012. Activation of neuronal P2X7 receptor-pannexin-1 mediates death of enteric neurons during colitis. Nat Med 18(4):600–604.

Hanani M, Reichenbach A. 1994. Morphology of horseradish peroxidase (HRP)-injected glial cells in the myenteric plexus of the guinea-pig. Cell Tissue Res 278(1):153–160.

Heanue TA, Pachnis V. 2007. Enteric nervous system development and Hirschsprung's disease: advances in genetic and stem cell studies. Nat Rev Neurosci 8(6):466–479.

Herbarth B, Pingault V, Bondurand N, Kuhlbrodt K, Hermans-Borgmeyer I, Puliti A, Lemort N, Goossens M, Wegner M. 1998. Mutation of the Sry-related Sox10 gene in Dominant megacolon, a mouse model for human Hirschsprung disease. Proc Natl Acad Sci USA 95(9):5161–5165.

Hoff S, Zeller F, von Weyhern CWH, Wegner M, Schemann M, Michel K, Ruhl A. 2008. Quantitative assessment of glial cells in the human and guinea rig enteric nervous system with an anti-sox8/9/10 antibody. J Comp Neurol 509(4):356–371.

Jessen KR. 2004. Glial cells. Int J Biochem Cell Biol 36(10):1861–1867.

Jessen KR, Mirsky R. 1980. Glial cells in the enteric nervous system contain glial fibrillary acidic protein. Nature 286(5774):736–737.

Joseph NM, He S, Quintana E, Kim YG, Nunez G, Morrison SJ. 2011. Enteric glia are multipotent in culture but primarily form glia in the adult rodent gut. J Clin Invest 121(9):3398–3411.

Laranjeira C, Sandgren K, Kessaris N, Richardson W, Potocnik A, Vanden Berghe P, Pachnis V. 2011. Glial cells in the mouse enteric nervous system can undergo neurogenesis in response to injury. J Clin Invest 121(9):3412–3424.

Lee JC, Mayer-Proschel M, Rao MS. 2000. Gliogenesis in the central nervous system. Glia 30(2):105–121.

Lemke G. 2001. Glial control of neuronal development. Annu Rev Neurosci 24:87–105.

MacEachern SJ, Patel BA, McKay DM, Sharkey KA. 2011. Nitric oxide regulation of colonic epithelial ion transport: a novel role for enteric glia in the myenteric plexus. J Physiol 589(Pt 13):3333–3348.

Matsuoka T, Ahlberg PE, Kessaris N, Iannarelli P, Dennehy U, Richardson WD, McMahon AP, Koentges G. 2005. Neural crest origins of the neck and shoulder. Nature 436(7049):347–355.

Nasser Y, Fernandez E, Keenan CM, Ho W, Oland LD, Tibbles LA, Schemann M, MacNaughton WK, Ruhl A, Sharkey KA. 2006a. Role of enteric glia in intestinal physiology: effects of the gliotoxin fluorocitrate on motor and secretory function. Am J Physiol Gastrointest Liver Physiol 291(5):G912–927.

Nasser Y, Ho W, Sharkey KA. 2006b. Distribution of adrenergic receptors in the enteric nervous system of the guinea pig, mouse, and rat. J Comp Neurol 495(5):529–553.

Nasser Y, Keenan CM, Ma AC, McCafferty DM, Sharkey KA. 2007. Expression of a functional metabotropic glutamate receptor 5 on enteric glia is altered in states of inflammation. Glia 55(8):859–872.

Neunlist M, Van Landeghem L, Mahe MM, Derkinderen P, des Varannes SB, Rolli-Derkinderen M. 2013. The digestive neuronal-glial-epithelial unit: a new actor in gut health and disease. Nat Rev Gastroenterol Hepatol 10(2):90–100.

Paratore C, Eichenberger C, Suter U, Sommer L. 2002. Sox10 haploinsufficiency affects maintenance of progenitor cells in a mouse model of Hirschsprung disease. Hum Mol Genet 11(24):3075–3085.

Perea G, Navarrete M, Araque A. 2009. Tripartite synapses: astrocytes process and control synaptic information. Trends Neurosci 32(8):421–431.

Pusch C, Hustert E, Pfeifer D, Sudbeck P, Kist R, Roe B, Wang Z, Balling R, Blin N, Scherer G. 1998. The SOX10/Sox10 gene from human and mouse: sequence, expression, and transactivation by the encoded HMG domain transcription factor. Hum Genet 103(2):115–123.

Ruhl A, Nasser Y, Sharkey KA. 2004. Enteric glia. Neurogastroenterol Motil 16(Suppl 1):44–49.

Sasselli V, Pachnis V, Burns AJ. 2012. The enteric nervous system. Dev Biol 366(1):64–73.

Savidge TC, Newman P, Pothoulakis C, Ruhl A, Neunlist M, Bourreille A, Hurst R, Sofroniew MV. 2007. Enteric glia regulate intestinal barrier function and inflammation via release of S-nitrosoglutathione. Gastroenterology 132(4):1344–1358.

Sofroniew MV. 2009. Molecular dissection of reactive astrogliosis and glial scar formation. Trends Neurosci 32(12):638–647.

Sofroniew MV, Vinters HV. 2010. Astrocytes: biology and pathology. Acta Neuropathol 119(1):7–35.

Srinivas S, Watanabe T, Lin CS, William CM, Tanabe Y, Jessell TM, Costantini F. 2001. Cre reporter strains produced by targeted insertion of EYFP and ECFP into the ROSA26 locus. BMC Dev Biol 1:4.

Stenkamp-Strahm C, Patterson S, Boren J, Gericke M, Balemba O. 2013. High-fat diet and age-dependent effects on enteric glial cell populations of mouse small intestine. Auton Neurosci 177(2):199–210.

Thacker M, Rivera LR, Cho HJ, Furness JB. 2011. The relationship between glial distortion and neuronal changes following intestinal ischemia and reperfusion. Neurogastroenterol Motil 23(11):e500–e509.

Tjwa ET, Bradley JM, Keenan CM, Kroese AB, Sharkey KA. 2003. Interleukin-1beta activates specific populations of enteric neurons and enteric glia in the guinea pig ileum and colon. Am J Physiol Gastrointest Liver Physiol 285(6):G1268–G1276.

Vanden Berghe P, Tack J, Boesmans W. 2008. Highlighting synaptic communication in the enteric nervous system. Gastroenterology 135(1):20–23.

Vanderwinden JM, Timmermans JP, Schiffmann SN. 2003. Glial cells, but not interstitial cells, express P2X7, an ionotropic purinergic receptor, in rat gastrointestinal musculature. Cell Tissue Res 312(2):149–154.

von Boyen GB, Steinkamp M, Reinshagen M, Schafer KH, Adler G, Kirsch J. 2004. Proinflammatory cytokines increase glial fibrillary acidic protein expression in enteric glia. Gut 53(2):222–228.

Young HM, Bergner AJ, Muller T. 2003. Acquisition of neuronal and glial markers by neural crest-derived cells in the mouse intestine. J Comp Neurol 456(1):1–11.

Zong H, Espinosa JS, Su HH, Muzumdar MD, Luo L. 2005. Mosaic analysis with double markers in mice. Cell 121(3):479–492.